CL-200064 Received: January 28, 2020 | Accepted: February 18, 2020 | Web Released: April 14, 2020

Cu(II) Porphyrin-catalyzed Coupling of Alkyl Tosylates and Grignard Reagents

Iori Matsuoka, Takuya Kurahashi,* and Seijiro Matsubara*
Department of Material Chemistry, Graduate School of Engineering, Kyoto University, Kyoto 615-8510, Japan

E-mail: kurahashi.takuya.2c@kyoto-u.ac.jp (T. Kurahashi), matsubara.seijiro.2e@kyoto-u.ac.jp (S. Matsubara)

Copper(II) porphyrin-catalyzed coupling of alkyl tosylates and alkyl Grignard reagents afforded substituted alkanes. The role of the copper(II) porphyrin complex was examined using EPR and *in-situ* synchrotron-based X-ray absorption fine structure measurements. These studies suggested that neither Cu redox nor substitution via *in-situ* generated cuprate was involved in catalysis. The results supported a reaction mechanism involving single electron transfer from copper(II) porphyrin to tosylate to facilitate the nucleophilic addition of Grignard reagents.

Keywords: Cross-coupling reaction | Electron-transfer | In-situ XAFS

Coupling reactions are one of the most important and versatile carbon–carbon bond-forming transformations in organic synthesis.[1] Continuous efforts have been made to develop transition metal-catalyzed sp^3–sp^3 coupling reactions, and there are currently a wide range of alkyl halides and pseudohalides available for use with a variety of organometallic reagents for this purpose.[2] Burns et al. and Cahiez et al. have shown that cuprate acts as a key intermediate for nucleophilic substitution with halide leaving groups in copper-catalyzed coupling reactions between alkyl halides and Grignard reagents.[3] Kambe and co-workers have developed copper-catalyzed cross-coupling reactions between alkyl halides and Grignard reagents, in which carbon–carbon bond formation occurred via reductive elimination at the copper metal center.[4,5] Furthermore, copper catalyzed reaction of higher alkyl halides including tertiary halides with allylic Grignard reagents were reported by Yorimitsu and Oshima.[6] In this communication, we describe the coupling of alkyl tosylates with Grignard reagents promoted by a copper porphyrin complex via an alternative reaction mechanism.

We initially found that secondary alkyl tosylate **1** reacted with secondary alkyl Grignard reagent **2** in the presence of the copper(II) porphyrin complex, CuTPP (Table 1, Entry 1). The reaction proceeded at 25 °C for 2 h to provide the sp^3–sp^3 coupling product in 64% yield. The product yield slightly decreased when the reaction was performed at −10 °C (Entry 2). Among the metalloporphyrin complexes examined, only copper(II) porphyrin promoted the reaction, with the cobalt(II), nickel(II), manganese(II), and zinc(II) complexes yielding only trace amounts of product (Entries 3–6). Mesityl-substituted copper(II) porphyrin, CuTMP, was also found to catalyze the reaction, although with a slight decrease in yield (60%). Copper(II) porphyrin-catalyzed coupling could also be applied to primary alkyl tosylates and tertiary Grignard reagents (Scheme 1). Primary alkyl tosylate **4** reacted with tertiary Grignard **5** in the presence of the copper(II) porphyrin complex to provide the sp^3–sp^3 coupling product **6** in 88% yield. Notably, product **6** failed to form in the absence of the copper(II) porphyrin complex, indicating that the catalyst is essential for the sp^3–sp^3 coupling of both the secondary alkyl tosylate with the secondary alkyl Grignard reagent and the primary alkyl tosylate with the tertiary alkyl Grignard reagent.

Table 1. Metalloporphyrin-catalyzed coupling reactions[a]

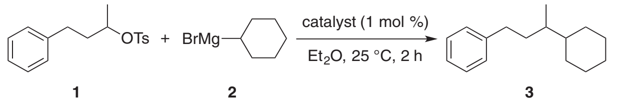

entry	catalyst	yield (%)
1	CuTPP	64
2	CuTPP	56[b]
3	CoTPP	<1
4	NiTPP	<1
5	MnTPP	<1
6	ZnTPP	<1
7	H_2TPP	<1
8	—	<1
9	CuTMP	60
10	CuTMP	23[b]

[a] Reaction conditions: catalyst (1 mol %), alkyl tosylate **1** (0.2 mmol), and CyMgBr **2** (0.4 mmol) in Et_2O (1 mL) at 25 °C for 2 h. TPP = *meso*-tetraphenylporphyrinato, TMP = *meso*-tetramesitylporphyrinato. [b] Reaction at −10 °C.

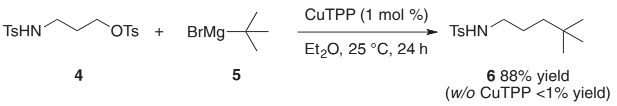

Scheme 1. Copper(II) porphyrin-catalyzed coupling reactions.

To obtain mechanistic information for this coupling reaction, we performed Cu K-edge X-ray absorption spectroscopy (XAS) (Figure 1).[7] Cu K-edge X-ray absorption near edge structure (XANES) spectra of the copper(II) porphyrin complex was obtained using Cu(0) foil, Cu(I) chloride, and Cu(II) dichloride as references. In contrast to Cu(0) foil (orange line) and Cu(I) chloride (black line), the main edge of copper(II) porphyrin (navy line) shifted to a higher energy with an increased oxidation state. Notably, the absorption edge energies (E_0) of Cu(II) dichloride and copper(II) porphyrin were almost identical (Table 2, Entries 3 and 7, respectively), indicating that the oxidation state of copper with the porphyrin ligand resembled that of Cu(II) dichloride. To compare the reaction mechanism of the previously reported Cu(II) dichloride/butadiene-catalyzed reaction with that of the copper(II) porphyrin-catalyzed reaction, we investigated the active species of the Cu(II) dichloride/butadiene catalyst. The solution-phase Cu K-edge XAS of Cu(II) dichloride and Cu(II) dichloride with either butadiene, CyMgBr, or both butadiene and CyMgBr in THF was measured (Figure 2). The addition of CyMgBr (navy line) led to remarkable changes in the pre-edge and main edge regions of

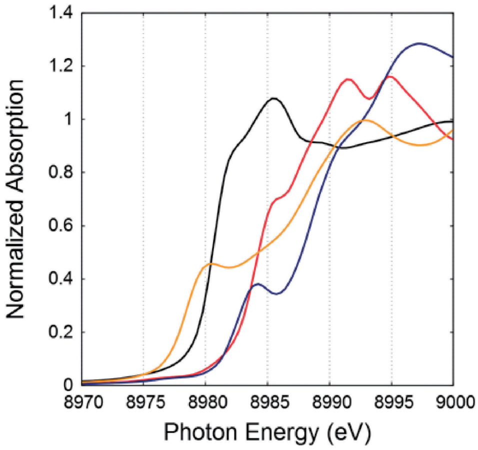

Figure 1. Solid-phase Cu *K*-edge XANES spectra (pellet): Cu(0) foil (orange line), CuCl (black line), $CuCl_2$ (red line), and CuTPP (navy line).

Table 2. Cu *K*-edge absorption energy (E_0)

entry	copper	E_0[a]
1	Cu foil	8978.4
2	CuCl	8984.0
3	$CuCl_2$	8988.5
4	$CuCl_2$/butadiene	8988.5
5	$CuCl_2$/CyMgBr	8986.9
6	$CuCl_2$/butadiene/CyMgBr	8987.4
7	CuTPP	8988.3
8	CuTPP/CyMgBr	8988.3

[a] Second peak of the first derivative of μ(E).

the XANES spectra as compared to Cu(II) dichloride (black line), confirming the reduction of Cu(II) to low-valent copper species. The addition of CyMgBr decreased the E_0 value of Cu(II) dichloride, further suggesting a decreased oxidation state (Table 2, Entries 3 and 5, respectively). It is noteworthy that the XANES spectra for the solution of Cu(II) dichloride with both butadiene and CyMgBr (orange line) is not identical to that of Cu(II) dichloride with CyMgBr (navy line), indicating that butadiene indeed coordinated to lower-valence copper species, as previously reported by Kambe and co-workers.[4d,8]

We next investigated the copper(II) porphyrin-catalyzed reaction using K-edge XAS, as it is ideal for identifying active copper species. The solution-phase Cu K-edge XAS of copper(II) porphyrin and copper(II) porphyrin with CyMgBr in THF were measured (Figure 3). There were no observable changes in the pre-edge or main edge regions of the copper(II) porphyrin XANES spectra (black line) upon addition of CyMgBr (red line), indicating that copper(II) was not reduced to a lower valence species when complexed to porphyrin. This was further confirmed by the identical E_0 values of the copper(II) porphyrin complex with and without added CyMgBr (Table 2, Entries 7 and 8, respectively).

X-ray absorption fine structure (EXAFS) analysis of the copper(II) porphyrin complex was performed with and without CyMgBr (Figure 4). The spectral features arising from the coordination sphere of the copper atoms, i.e., the radial distance,

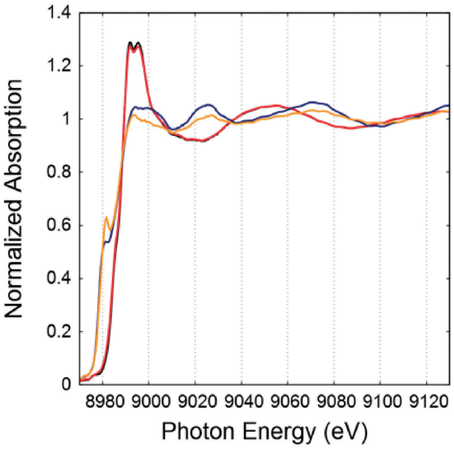

Figure 2. Solution-phase Cu *K*-edge XANES spectra: $CuCl_2$ (black line), $CuCl_2$ with butadiene (red line), $CuCl_2$ with CyMgBr (navy line), and $CuCl_2$ with butadiene and CyMgBr (orange line).

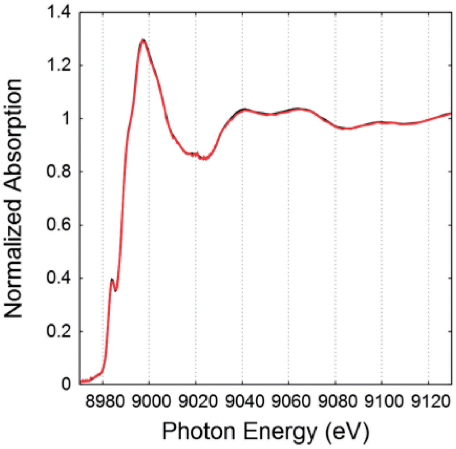

Figure 3. Solution-phase Cu *K*-edge XANES spectra: CuTPP (black line) and CuTPP with CyMgBr (red line).

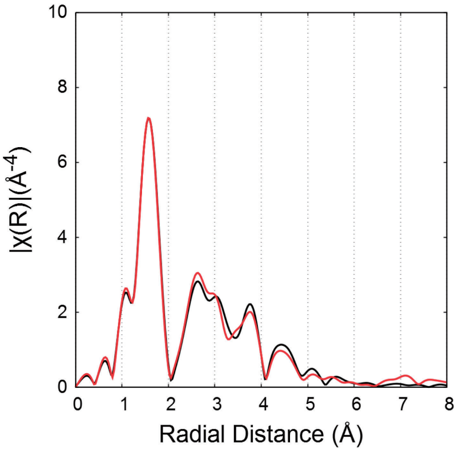

Figure 4. Solution-phase Cu *K*-edge EXAFS analysis (Fourier transform of k^3-weighted spectrum): CuTPP (black line) and CuTPP with CyMgBr (red line).

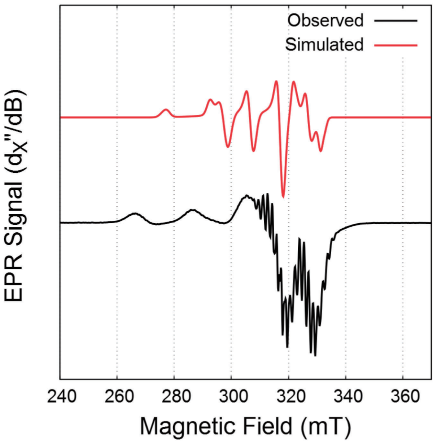

Figure 5. X-Band EPR spectrum of CuTPP in frozen THF at 77 K (black line) and simulated spectrum (red line). EPR experimental parameters: microwave frequency = 9.104859 GHz, power = 0.998 mW, modulation amplitude = 0.1 mT.

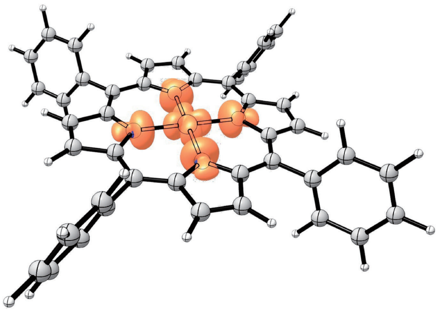

Figure 6. Spin density plot of CuTPP calculated with DFT [CPCM(THF)-B3LYP/def2-TZVP//CPCM(THF)-B3LYP-D3/Lanl2dz(f)(Cu), 6-31G(d)(else)].

were similar for the copper(II) porphyrin solutions with and without CyMgBr. These results clearly suggest that copper(II) porphyrin does not react with CyMgBr to afford either low-valent copper species or cuprate reagents.

To further investigate the catalytically active species involved in the coupling reaction, X-band electron paramagnetic resonance (EPR) spectroscopy was measured for the copper(II) porphyrin catalyst at 77 K.[9] A frozen solution of the copper(II) porphyrin catalyst displayed a signal characteristic for radical species (Figure 5). This finding was in agreement with the simulated EPR spectrum obtained using the DFT-calculated EPR parameters for the corresponding copper(II) porphyrin model (Figures 6).

To examine the stereochemistry of the copper(II) porphyrin-catalyzed coupling reaction during formation of the carbon–carbon bond and thereby elucidate the reaction mechanism, chiral tosylate **7** was reacted with Grignard reagent **2** (Scheme 2). The copper-catalyzed coupling of alkyl halides and tosylates with Grignard reagents has previously been shown to proceed via nucleophilic substitution type stereochemistry. Coupling product **8** was obtained in 99% *ee* with inversion of configuration at the newly formed carbon–carbon bond, confirming that this reaction also proceeded via a nucleophilic substitution type mechanism with respect to both the elimination of the leaving group and formation of the carbon–carbon bond. In addition, coupling between secondary alkyl tosylate **9** and tertiary alkyl Grignard **5** provided **10** in lower yield compared to that of secondary alkyl tosylate **1** with secondary alkyl Grignard **2** or primary alkyl tosylate **4** with tertiary alkyl Grignard **5**. This influence of steric hindrance on the reaction productivity further supports a nucleophilic substitution type mechanism.

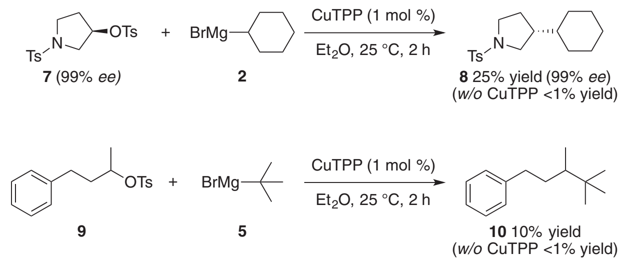

Scheme 2. Nucleophilic substitution type substitution coupling reactions.

Based on this work, we propose a catalytic reaction mechanism involving initial single electron transfer (SET) from copper(II) porphyrin to alkyl tosylate, which is coordinated to the Lewis acidic magnesium of the Grignard reagent. Subsequent nucleophilic substitution type addition of the activated Grignard carbanion via SET, which enhances the Lewis basicity of the oxygen atom coordinated to magnesium, forms the carbon–carbon bond. The tosylate moiety and copper(II) porphyrin catalyst are then regenerated through a second SET between the tosyl radical and copper(II) porphyrin to form tosyl magnesium bromide.[10]

In summary, we developed a copper(II) porphyrin-catalyzed coupling reaction between nonactivated alkyl tosylates and alkyl Grignard reagents. The reaction proceeded via formal nucleophilic substitution type addition with inversion of stereochemistry upon leaving group elimination and carbon–carbon bond formation. A mechanistic investigation revealed that the reaction did not proceed via a cuprate intermediate or low-valent copper species, as had been reported for previous Cu-catalyzed coupling reactions. This coupling reaction may provide new insight into transition and non-transition metal-catalyzed coupling reactions. Further experimental and theoretical investigations into the reaction mechanism are underway and will be reported in due course.[11]

This work was supported by Grant-in-Aid for Scientific Research (Nos. 18H04253 and 17KT0006) from the Ministry of Education, Culture, Sports, Science and Technology (Japan). We thank Dr. Tetsuo Honma and Dr. Hironori Ofuchi (JASRI: Japan Synchrotron Radiation Research Institute), and Mr. Kyohei Fujiwara (Ajinomoto Co., Inc.) for their valuable help with X-ray absorption fine structure analysis. A portion of this study was performed at the BL14B2 beamline of the SPring-8 synchrotron radiation facility with the approval of the Japan Synchrotron Radiation Research Institute (Proposal Nos. 2015B1770, 2016A1549, 2016A1680, 2016B1766, 2017A1700, 2017B1748, 2018A1690, 2018B1594, 2019A1712, and 2019B1842).

Supporting Information is available on https://doi.org/10.1246/cl.200064.

References and Notes

1 a) *Metal-Catalyzed Cross-Coupling Reactions*, 2nd ed., ed. by A. de Meijere, F. Diederich, Wiley-VCH, Weinheim, **2004**. b) *Metal-catalyzed Cross-Coupling Reactions*, 1st ed., ed. by F. Diederich, P. J. Stang, Wiley-VCH, Weinheim, **1998**. For selected reviews on metal-catalyzed cross-coupling reactions, see: c) R. Jana, T. P. Pathak, M. S. Sigman, *Chem. Rev.* **2011**, *111*, 1417. d) W.-T. T. Chang, R. C. Smith, C. S. Regens, A. D. Bailey, N. S. Werner, S. E. Denmark, *Org. React.* **2011**, *75*, 213. e) Y. Nakao, T. Hiyama, *Chem. Soc. Rev.* **2011**, *40*, 4893. f) H. F. Sore, W. R. J. D. Galloway, D. R. Spring, *Chem. Soc. Rev.* **2012**, *41*, 1845.

2 a) T. Iwasaki, N. Kambe, in *Comprehensive Organic Synthesis*, 2nd ed., ed. by P. Knochel, G. A. Molander, Elsevier, Oxford, **2014**, Vol. 3, pp. 337–391. For selected reviews on metal-catalyzed sp^3–sp^3 cross-coupling reactions, see: b) D. J. Cárdenas, *Angew. Chem., Int. Ed.* **2003**, *42*, 384. c) M. R. Netherton, G. C. Fu, *Adv. Synth. Catal.* **2004**, *346*, 1525. d) A. C. Frisch, M. Beller, *Angew. Chem., Int. Ed.* **2005**, *44*, 674. e) A. Rudolph, M. Lautens, *Angew. Chem., Int. Ed.* **2009**, *48*, 2656. f) N. Kambe, T. Iwasaki, J. Terao, *Chem. Soc. Rev.* **2011**, *40*, 4937. g) X. Hu, *Chem. Sci.* **2011**, *2*, 1867. h) S. Thapa, B. Shrestha, S. K. Gurung, R. Giri, *Org. Biomol. Chem.* **2015**, *13*, 4816. i) J. Choi, G. C. Fu, *Science* **2017**, *356*, eaaf7230.

3 a) D. H. Burns, J. D. Miller, H.-K. Chan, M. O. Delaney, *J. Am. Chem. Soc.* **1997**, *119*, 2125. b) G. Cahiez, C. Chaboche, M. Jézéquel, *Tetrahedron* **2000**, *56*, 2733. c) G. Cahiez, O. Gager, J. Buendia, *Synlett* **2010**, 299.

4 a) J. Terao, A. Ikumi, H. Kuniyasu, N. Kambe, *J. Am. Chem. Soc.* **2003**, *125*, 5646. b) J. Terao, H. Todo, S. A. Begum, H. Kuniyasu, N. Kambe, *Angew. Chem., Int. Ed.* **2007**, *46*, 2086. c) J. Terao, N. Kambe, *Acc. Chem. Res.* **2008**, *41*, 1545. d) R. Shen, T. Iwasaki, J. Terao, N. Kambe, *Chem. Commun.* **2012**, *48*, 9313.

5 a) C.-T. Yang, Z.-Q. Zhang, J. Liang, J.-H. Liu, X.-Y. Lu, H.-H. Chen, L. Liu, *J. Am. Chem. Soc.* **2012**, *134*, 11124. b) P. Ren, L.-A. Stern, X. Hu, *Angew. Chem., Int. Ed.* **2012**, *51*, 9110. c) R. Shinohara, M. Morita, N. Ogawa, Y. Kobayashi, *Org. Lett.* **2019**, *21*, 3247.

6 a) M. Sai, H. Someya, H. Yorimitsu, K. Oshima, *Org. Lett.* **2008**, *10*, 2545. b) M. Sai, H. Yorimitsu, K. Oshima, *Bull. Chem. Soc. Jpn.* **2009**, *82*, 1194.

7 An oxygen- and moisture-proof, adjustable-thickness liquid sample cell was designed and developed for the *in-situ* XAFS measurements performed at the SPring-8 synchrotron radiation facility.

8 T. Iwasaki, R. Imanishi, R. Shimizu, H. Kuniyasu, J. Terao, N. Kambe, *J. Org. Chem.* **2014**, *79*, 8522; For a review on the effects of olefins on transition-metal-catalysts, see: J. B. Johnson, T. Rovis, *Angew. Chem., Int. Ed.* **2008**, *47*, 840.

9 EPR spectra were simulated using EasySpin for MATLAB with DFT calculated EPR parameters without fitting procedures ($g_{//\mathrm{calc}} = 2.163$, $g_{\perp\mathrm{calc}} = 2.077$). The g values from ENDOR measurements for CuTPP are $g_{//} = 2.190$ and $g_{\perp} = 2.045$. a) M. Iwaizumi, Y. Ohba, H. Iida, M. Hirayama, *Inorg. Chim. Acta* **1984**, *82*, 47. b) T. G. Brown, B. M. Hoffman, *Mol. Phys.* **1980**, *39*, 1073. c) C. Calle, A. Schweiger, G. Mitrikas, *Inorg. Chem.* **2007**, *46*, 1847.

10 For examples on SET-induced coupling reactions of alkenyl and aryl halides with Grignard reagents, see: a) E. Shirakawa, R. Watabe, T. Murakami, T. Hayashi, *Chem. Commun.* **2013**, *49*, 5219. b) N. Uchiyama, E. Shirakawa, T. Hayashi, *Chem. Commun.* **2013**, *49*, 364. c) E. Shirakawa, T. Hayashi, *Chem. Lett.* **2012**, *41*, 130. d) E. Shirakawa, K. Okura, N. Uchiyama, T. Murakami, T. Hayashi, *Chem. Lett.* **2014**, *43*, 922.

11 Additional examples for the CuTPP-catalyzed couplings are briefly summarized in the Supporting Information.